

Research Article

Investigation of the Distribution of EAB 515 to Cortical ECF and CSF in Freely Moving Rats Utilizing Microdialysis

Bimal K. Malhotra,¹ Michel Lemaire,² and Ronald J. Sawchuk^{1,3}

Received December 3, 1993; accepted April 26, 1994

A freely moving rat model was developed to study the CNS distribution of EAB 515 (S- α -amino-5-phosphonomethyl[1,1'-biphenyl]-3-propanoic acid). Microdialysis (MD) in the frontal cortex (FrC) and in the lateral ventricle (LV) of the rat brain was performed to measure the levels of EAB 515 in the cortical extracellular fluid (ECF) as well as in the cerebrospinal fluid (CSF). The femoral artery and femoral vein were cannulated for serial blood sampling and intravenous (iv) drug administration, respectively. EAB 515 was also administered *via* the intracerebroventricular (icv) route in a cross-over experiment. The *in vivo* recovery of EAB 515 across the MD probes was determined by simultaneous retrodialysis (RD) performed using a hydroxylated analog of EAB 515, as the RD calibrator (RDC). An extremely sensitive and selective on-line HPLC system with native fluorescence detection was developed for the simultaneous analysis of EAB 515 and RDC in microdialysate samples from rat CSF and cortical ECF. Unbound concentrations of EAB 515 in the rat plasma were determined by direct injection of plasma ultrafiltrate onto the HPLC column. The validity of the use of RDC as the RD calibrator was demonstrated by comparing the results of zero-net flux (ZNF) analysis simultaneously in some experiments. After constant rate iv infusion in rats ($n = 12$) for 900 min, the average (S.D.) ratio of the levels of EAB 515 in the CSF to those in plasma ($C_{\text{CSF,iv}}/C_p$) was determined to be 17.7 (7.8)% and that in the cortex relative to plasma ($C_{\text{cortex,iv}}/C_p$) was 8.3 (4.8)%. In these animals the total body clearance (Cl) of EAB 515 was estimated to be 8.5 ± 1.6 ml/min/kg. Upon icv administration in the lateral ventricle of rats ($n = 6$), a 136 ± 42 -fold distribution advantage in the cortical ECF was determined. These results indicate a significant contribution from the transport across the CSF-Brain interface to the total uptake of EAB 515 by cortical tissue.

KEY WORDS: brain microdialysis; zero-net flux; retrodialysis; EAB 515; NMDA antagonist; rat; intracerebroventricular administration; distribution advantage; clearance; probenecid.

INTRODUCTION

The excitatory amino acids, glutamate and aspartate, are known to act as neurotransmitters at three types of receptors within the central nervous system (CNS), *viz.*, N-methyl-D-aspartate (NMDA), quisqualate, and kainate receptors (1). The distribution of these receptors in rat brain is heterogeneous, with high densities found in the hippocampus and the frontal cortex (2).

EAB 515 is an experimental NMDA antagonist which exhibits much greater potency *in vivo* than the previously available antagonists such as 2-APH, 2-APV, D-CPP, and D-CPPene (3). The fact that EAB 515 is very polar and yet has an appreciable access to brain tissue makes it an interesting candidate for the mechanistic investigation of its CNS distribution across the blood-brain barrier (BBB), blood-CSF barrier (BCB), and the CSF-brain interface (CBI). This

study is designed to investigate possible transport pathways for EAB 515 across the BBB, BCB and the CBI, and their relative contribution in its access to regions of the brain. Furthermore, the knowledge of the mechanism(s) involved in transport of a drug across the BBB, BCB, and/or CBI is of importance in order that transport profiles may be optimized by molecular modification (4) or by adjunct therapy (5).

THEORETICAL

Relative Recovery Across Microdialysis Probes

The process of microdialysis represents a non-equilibrium situation. The concentration ($C_{e,s}$) of the dialyzed solute in the microdialysate is only a fraction of its concentration ($C_{o,s}$) in the medium that is being dialyzed. The relationship between $C_{o,s}$ and $C_{e,s}$ is defined by equation 1 as relative recovery, R_s .

$$R_s = C_{e,s}/C_{o,s} \quad (1)$$

In an *in vivo* microdialysis experiment, however, $C_{o,s}$ as well as R_s are unknown variables. Therefore, in order to characterize the drug concentration in the tissue space being dialyzed in a pharmacokinetic study, it becomes necessary to

¹ Department of Pharmaceutics, College of Pharmacy, University of Minnesota, Minneapolis, MN 55455.

² Biopharmaceutical Department, Sandoz Pharma Ltd, CH-4002 Basel, Switzerland.

³ To whom correspondence should be addressed.

obtain an estimate of relative recovery of the drug *in vivo*. The inherent differences in the diffusive behavior of a solute in the ECF of the dialyzed tissue and in water typically result in significantly different recovery values *in vivo* and *in vitro*.

Several approaches have been reported in the microdialysis literature for estimation of the recovery of solutes in an *in vivo* microdialysis experiment. A steady-state mass transfer relationship has been used by Jacobson et al. (6) to characterize the flow rate dependence of the dialysate concentration, $C_{e,s}$. This is called the "flow-rate" or "stop-flow" method. Lonroth et al. (7) developed a method where the *in vivo* recovery is estimated from dialysate concentrations when a wide range of concentrations ($C_{i,s}$) of the solute of interest are perfused, while maintaining the ECF concentration at steady state. This is referred to as the "concentration difference" method or "zero-net flux" method. Wang et al. (8) proposed the use of a closely related analog of the solute as a calibrator in the microdialysis perfusate. The loss of the calibrator during perfusion is measured and the value is used to estimate the *in vivo* recovery of the drug. This method of "retrodialysis" and the zero-net flux method have been used simultaneously for microdialysis calibration, and it was concluded that both gave comparable results (9).

Distribution Advantage

The term "distribution advantage" essentially evaluates the relative uptake of a drug by a peripheral compartment when the drug is administered into another peripheral compartment *vis-a-vis* into the central compartment. The distribution advantage for a drug may occur only if there exists a transport pathway between the two peripheral compartments (see Figure 1). In the present study plasma, cortical ECF, and CSF may be considered to be parts of the central compartment and the peripheral compartments 1 and 2, re-

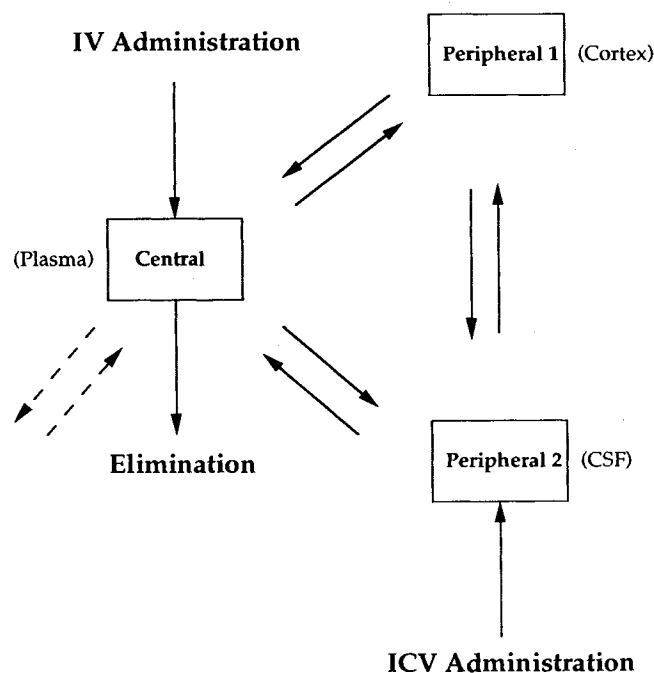


Fig. 1. Strongly connected compartmental model for distribution of EAB 515 during iv and icv administration.

spectively. At steady state, if the ratio of cortical ECF concentration to plasma concentration of a drug (C_{cortex}/C_p) is higher when infused into the ventricle than into the systemic circulation, it may be concluded that icv administration offers a definite distribution advantage for the drug's uptake by the cortex. Therefore, a transport pathway between the cortical ECF and CSF may exist for that drug. Mathematically, distribution advantage (DA) may be defined as follows:

$$DA = \frac{(C_{\text{cortex,icv}}/C_{\text{cortex,iv}})_{ss}}{\times (\text{iv infusion rate/icv infusion rate})} \quad (2)$$

Equation 2 normalizes any difference in the infusion rate of drug by the two routes. The validity of this normalization is dependent upon the linearity of the different first-order processes involved in the kinetics of drug distribution.

MATERIALS AND METHODS

Drugs and Reagents

EAB 515 and its hydroxylated analog, RDC, were provided by Sandoz Pharma Ltd., Switzerland. Simulated CSF solution was made to give a final concentration of 1.1 mM Mg^{+2} , 144.2 mM Na^{+} , 1.35 mM Ca^{+2} , 129.5 mM Cl^{-1} , 3.0 mM K^{+1} , and 0.242 mM PO_4^{-3} at a pH of 7.6 (10). Drug solutions were prepared in Sorensen's pH 7.4 buffer for iv infusion and in artificial CSF for icv infusion. Solutions of EAB 515 and of RDC were made in simulated CSF for perfusion through the probes in the RD and ZNF experiments. All solvents used for HPLC and for perfusion through the probes were degassed by sonication for 15 minutes and filtered through polycarbonate membrane of 0.2 μm pore size (Costar, CA). Trifluoro acetic acid (99% pure) was obtained from Janssen Chimica, Belgium.

Probes

Microdialysis probes (CMA-12; BAS, West Lafayette, IN) were used as the sampling device for measuring the cortical and ventricular concentrations of EAB 515. The probes used in the FrC region had a dialysis membrane length of 2 mm and those in the LV were 1 mm long. The dialysis membrane had a 20,000-Dalton molecular weight cutoff, 400 μm ID and 500 μm OD. FEP tubing (with a dead volume of 12 $\mu\text{l}/\text{meter}$) and tubing connectors from BAS were used to connect the inlet and the outlet ports of the probes to the on-line microdialysis system.

Surgery

Male Sprague-Dawley (Harland Sprague-Dawley, IN) rats weighing approximately 300 g were used for this study. The animals were housed in the animal facilities area for a minimum of five days for acclimatization prior to performing any surgical operation on them. During acclimatization and post-operative recovery periods the animals were provided alternating dark/light cycles of 12 hrs each. At all times, including the duration of experiments, they had free access to food and water. Surgical preparation of these animals was done under aseptic conditions in two phases, each followed by a recovery period of a minimum of 48 hrs. Brain surgery was performed in the first phase and the cannulation of ar-

tery and vein in the second. All surgical procedures were performed after anesthesia using an i.p. dose of 65 mg/kg sodium pentobarbital (Anpro Pharmaceutical, CA). The first dose of anesthetic was followed by an i.p. dose of 0.04 mg atropine sulfate (LyphoMed Inc., IL). Brevital sodium (Lilly, IN) doses of 15 mg/kg were given i.p. to maintain anesthesia, if required. An i.m. dose of 30,000 units procaine penicillin G (Vedco, MO) was given following each surgery. After completion of the entire experiment, the animals were euthanized by giving 50 mg sodium pentobarbital intravenously.

Implantation of the Guide Cannulae for Microdialysis Probes

The anaesthetized animal was placed on its ventral surface on the stereotaxic instrument model 1504 with a rat adaptor (David Kopf Instruments, CA). Two ear bars were positioned firmly in the auditory meatus on either side of the head. Correct placement and rigid mounting allowed movement of the head only in the ventral direction. The teeth were mounted on the incisor bar and the nose clamp was tightened. The head was shaved and a 2 to 3-cm long incision was made in the scalp along the midline. The periosteal connective tissue that adheres to the bone was removed in order to expose the cranial sutures. The bregma and lambda were located on the skull. The ventral coordinates of the bregma and the lambda were checked successively to make any required adjustments in the height of the incisor bar, for a precisely horizontal skull surface.

The coordinates for the FrC and the LV were determined from the rat stereotaxic atlas (11). All anteroposterior and lateral measurements were taken relative to the bregma, and the ventral measurements were taken from the brain surface. The FrC was located at 3.2 mm anterior, 1.2 mm lateral on the left, and 1.0 mm ventral. Corresponding coordinates for the LV were 0.9 mm posterior, 1.5 mm lateral on the right, and 3.0 mm ventral.

A hand held drill with Emesco engine model 503D (Tele-dyne Hanau, NY) was used to drill the holes approximately 1 mm in diameter. The vernier scales on the micro-electrode manipulators (David Kopf Instruments, CA) were used to locate the sites and to precisely insert the guide cannulae in the drilled holes at the desired depth. Dental cement (L. D. Caulk Company, DE) was used to anchor and fix the guide cannulae in place. Three stainless steel precision screws (Lomat Inc., Canada) were also drilled into the skull surface to a depth of approximately 1-mm for additional anchorage of the dental cement to the skull.

Cannulation of Femoral Artery and Femoral Vein

A 2-cm long incision was made in the upper thigh region of the rat's leg in order to expose the femoral artery and vein. The fascia around the vessels was removed by tearing with the help of micro-dissecting curved forceps. Approximately 1-cm long segments of the blood vessels were separated from each other and from the bundle of nerve fibers that are fused with the artery wall. Damage to the nerves was avoided so as not to impair the animal's mobility after recovery from the surgery. The isolated arterial segment was tied off at the distal end with surgical silk and the proximal end was

clamped off with the help of an artery clamp. The cannulae were made with a 50-cm long PE-50 (Clay Adams, NJ) tubing thermally fused end-to-end with a length of PE-10 tubing (3.5 cm for artery and 4.5 cm for the vein). A small transverse nick was made in the artery close to the distal end and the PE-10 end of the cannula was inserted into the vessel. The clamp was released in order to assist further insertion until the entire 3.5 cm length was in the artery. Blood flow was checked in the cannula and the line was kept in 50 U/ml heparinized saline solution in order to prevent blood clotting. The proximal end of the cannulated vessel was tied off to secure the cannula in place.

The same procedure was followed for cannulating the adjacent femoral vein, except that the proximal end of the vein was not clamped prior to nicking the vessel. The two cannulae were sewn onto the thigh muscle, and run up along the back under the skin to exit near the neck, where their bases were cemented into the microdialysis probe area on the head. The free ends of cannulae along with the four pieces of MD tubing were housed inside a flexible tether, which was anchored to the cement dam on the head with the help of embedded nylon screws.

During an experiment, the animal cage was set on a rotating platform. The six lengths of tubing were prevented from entanglement resulting from the animal's twisting motion in one given direction, by rotating the platform in the opposite direction, and keeping the external ends of the lines pivoted to a stationary support.

Comparison of Microdialysis Recovery Estimated by RD and ZNF

All *in vitro* microdialysis experiments were conducted at room temperature. The analysis of microdialysate samples was performed on-line. The CMA-12 probes were prepared for use in an experiment, according to the manufacturer's instructions. All solutions used for MD were prepared in simulated CSF. Probes were equilibrated in a 1000 ng/ml reservoir solution of EAB 515 with a 1000 ng/ml solution of RDC perfused through them at 0.4 μ l/min for at least one hour. At least six microdialysate samples were collected over 20-minute intervals in order to compute the retrodialysis recovery and loss of EAB 515 and RDC, respectively. The construction of a standard curve for EAB 515 and measurement of the perfusate inlet and the reservoir concentrations was done in the "bypass" mode. In "bypass" mode the solutions were pumped into the injection loops under identical conditions, without passing through the probes. For the estimation of recovery by zero-net flux, four different concentrations of EAB 515 were also incorporated into the perfusate solutions. Four microdialysate samples were analyzed at each of the concentrations. Thus data for recovery by RD as well as ZNF was obtained from the same set of experiments.

For *in vivo* experiments, the obturators were removed from the guide cannulae in the awake rat, and were replaced by CMA-12 probes that were perfused with blank simulated CSF at 0.4 μ l/min. The probes were equilibrated for 1–2 hrs and then a zero-order infusion of EAB 515 was started into the cannulated femoral vein of the rats. The microdialysate samples were monitored for the absence of any endogenous

peaks that might elute with the peaks of interest. At 2 hrs into the iv infusion, MD perfusion solution was switched to a 1000 ng/ml solution of RDC. After 12 hrs into the infusion, different concentrations of EAB 515 were successively introduced in the calibrator solution for the estimation of recovery by ZNF. Experimental details were similar to the *in vitro* section, except that the probes were in the CSF and the cortical ECF, respectively, while the animal was receiving drug by iv infusion, rather than being inserted in a beaker of drug solution.

Determination of Free Fraction of EAB 515 in Rat Plasma

Blank plasma from two rats and distilled water were spiked with accurately measured aliquots of EAB 515 stock solutions in order to obtain the desired concentrations of EAB 515 in plasma and in water. The spiked plasma solutions were placed in the top portion of the Centrifree model 4104 (Amicon, MA) apparatus and centrifuged at the blood setting of the Triac (Clay Adams, NJ) centrifuge for 10 minutes. The plasma ultrafiltrate from the receptacle was transferred to HPLC vials and analyzed for EAB 515 concentration according to the procedure described in the sample analysis section. The spiked aqueous solutions were directly analyzed for their EAB 515 content. The ratio of peak heights of EAB 515 in the spiked plasma ultrafiltrate and spiked aqueous samples was used as a measure of the free fraction (fu) of EAB 515 at different concentrations.

Determination of Cortical ECF to Plasma and CSF to Plasma Ratio upon IV Administration of EAB 515

A total of 12 rats were infused with EAB 515 into the femoral vein for 15 hrs. An accurately measured concentration of EAB 515 in Sorensen's pH 7.4 buffer was infused at 5 $\mu\text{l}/\text{min}$. During the iv infusion at a constant rate (R_{iv}) of 21–69 $\mu\text{g}/\text{min}$ and for 5 hours post-infusion, continuous MD sampling of the cortical ECF and the CSF was performed. 300 μl of blood was collected into heparinized tubes from the femoral artery, at 4, 6, 10, 12, and 15 hrs into the infusion, and then at 40, 80, 120, 160, 200, 240, and 300 minutes post-infusion. Plasma was immediately harvested and frozen until analysis. The experimental details of microdialysis were similar to those described under "Comparison of Microdialysis Recovery Estimation by RD and ZNF".

Determination of the Distribution Advantage in the Cortical ECF upon ICV Administration of EAB 515

Probes positioned in the cortex were perfused with simulated CSF at 0.4 $\mu\text{l}/\text{min}$ for an hour. The ventricular obturator was replaced by a 1 mm-tip CMA-12 probe with its membrane removed and the outlet port sealed off. EAB 515 solution in CSF was infused into it at 0.4 $\mu\text{l}/\text{min}$ to target an icv infusion rate (R_{icv}) of 10 or 20 ng/min for 15 hours. The perfusion through the cortical probe was immediately switched to a solution of the RD calibrator. Plasma samples were not collected during the icv infusion due to analytical sensitivity problems at the low infusion rates. The cortical microdialysate samples were collected directly into the injection loop for on-line analysis.

Inhibition of the Facilitated Transport of EAB 515 by Probenecid

A back-to-back cross-over experiment was designed. In the control phase, EAB 515 was infused intravenously for 12 hrs at 24–25 $\mu\text{g}/\text{min}$. This was immediately followed by a treatment phase of 12 hrs during which probenecid was coadministered (75 $\mu\text{g}/\text{min}$) with EAB 515. During the two phases, concentration of EAB 515 in the CSF and cortical ECF was monitored by MD, and blood samples were collected at 4, 6, 8, 10, 12, 15, 18, 21 and 24 hrs following the beginning of first phase.

Sample Analysis

Analysis of Plasma Ultrafiltrates

Plasma samples were subjected to ultrafiltration in an Amicon Centrifree apparatus. A 10- μl volume of the plasma ultrafiltrate was injected directly on the Maxsil-5 RP-2 column (Phenomenex, CA). Resolution of the EAB 515 peak from the endogenous peaks was attained by using a 0.09% solution of TFA in distilled water as mobile phase pumped at 1 ml/min. Peaks were monitored using a fluorescence detector (Shimadzu RF-535) on the low sensitivity setting. Wavelengths were set at 255 nm for excitation and 320 nm for emission. Integration of the peaks in terms of height was achieved on an HP-3396 integrator. Free concentrations of the drug in plasma were determined by regression of peak heights generated from analysis of an aqueous standard curve. The standard curve was found to be linear in the range of 20–10,000 ng/ml.

On-Line Analysis of Microdialysate Samples

Microdialysate samples from the two sites in the brain were collected directly in two injection loops of 5 μl capacity during alternating intervals of 20 minutes each. These samples were injected on column with chromatographic conditions identical to those described for plasma ultrafiltrate analysis. Standard curves were constructed in the concentration range of 5–2000 ng/ml. The studies were conducted on one of two similar on-line systems (Figure 2). One of these used a Waters 510 HPLC pump, Jasco FP-821 fluorescence detector (Att. 1; Gain x100) and a Spectra Physics 4290 integrator. The other employed a Shimadzu LC-10AD HPLC pump, Shimadzu RF-535 fluorescence detector (high sensitivity) and HP-3396 integrator. The time programming to control the collection intervals, loop switching, sample injection, and to start the integrator was achieved using a Valco digital valve sequence programmer model DVSP2 (VICI, TX). The injection loops were fitted into a 10-port Valco valve body model E 36 (VICI, TX).

RESULTS

Comparison of Microdialysis Recovery Estimated by RD and ZNF

Figure 3 shows a plot of the recovery of EAB 515 and the loss of RDC determined from the *in vitro* retrodialysis study at a flow rate of 0.4 $\mu\text{l}/\text{min}$. The data for all the probes fell close to the line of identity. An average (S.D.) value of

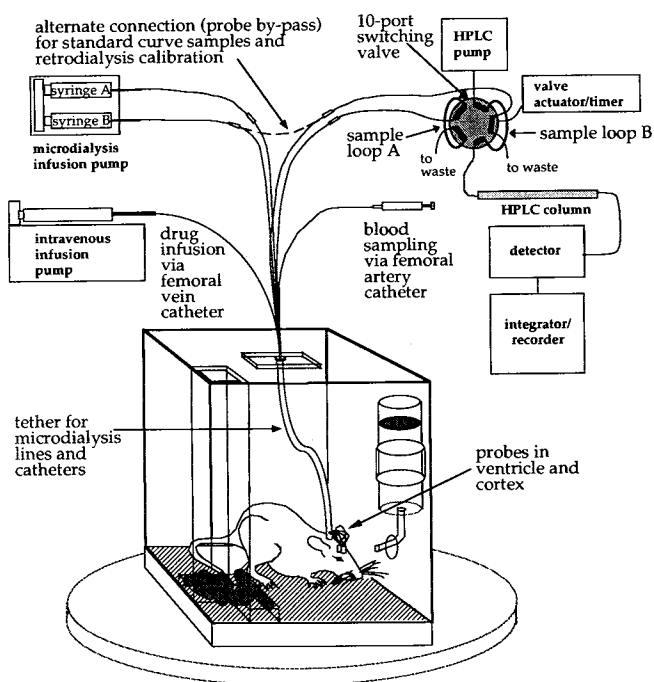


Fig. 2. Set-up of an on-line HPLC system for microdialysis in the freely moving rat.

1.07 (0.12) was determined for the ratio of loss and recovery of RDC and EAB 515, respectively (n = 20). *In vitro* zero-net flux measurement of the recovery for some of the probes was obtained and found to be in good agreement with the corresponding RD results. That these methods agreed supported the use of RDC as a RD calibrator for determining the recovery of EAB 515 at least in the *in vitro* experiments.

Figure 4 shows plots of the *in vivo* determination of recovery from CMA-12 probes implanted in the FrC and the LV of a rat that was being infused with EAB 515 into the femoral vein. In the FrC, both RD and ZNF gave comparable values for the recovery of EAB 515 (11.9% and 14.4%, re-

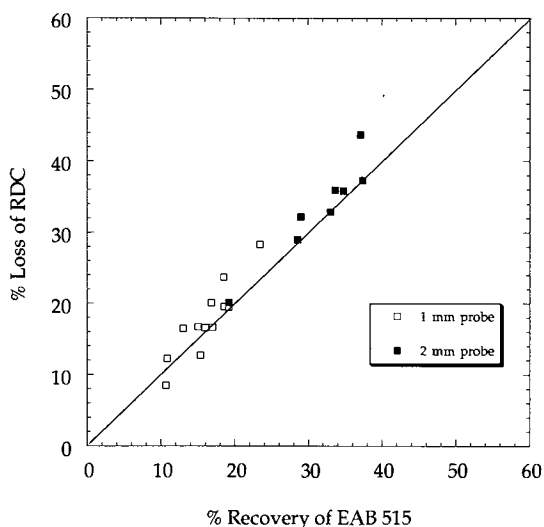


Fig. 3. *In vitro* relationship between loss of RDC and recovery of EAB 515 for retrodialysis. Mean values of six microdialysate samples for each probe, and the line of identity are shown.

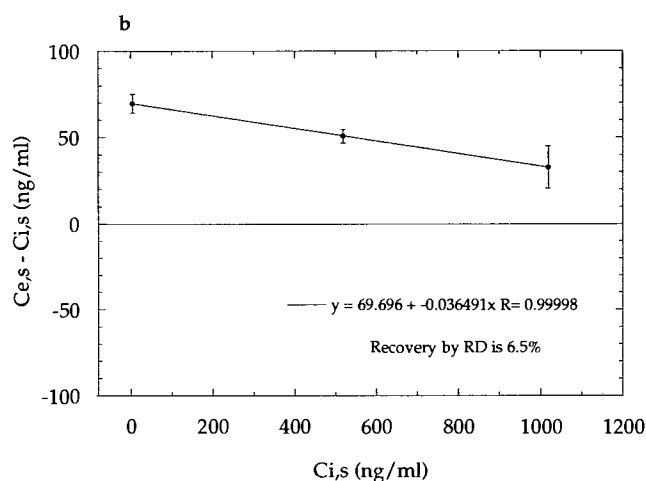
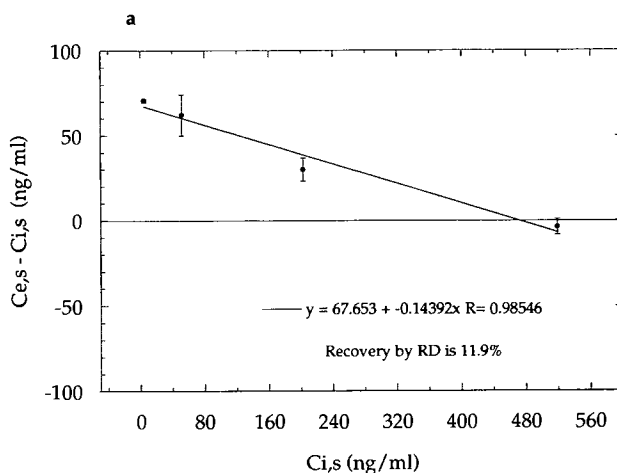


Fig. 4. Results of *in vivo* microdialysis in the frontal cortex (panel a) and lateral ventricle (panel b) of rat using simultaneous ZNF and RD for the estimation of recovery. The slope of the regression line is equal to the recovery of EAB 515.

spectively). However, in the LV the recovery of the probe determined by ZNF method (3.6%) was considerably lower than the recovery computed from RD (6.5%). Similar results for comparative ZNF and RD were obtained in two other animals.

Determination of Free Fraction of EAB 515 in Rat Plasma

The *in vitro* free fraction of EAB 515 in rat plasma was determined by ultrafiltration. For a wide range of concentrations of EAB 515 (100–10,000 ng/ml), the average free fraction was found to be 0.70. This value was used to calculate the total concentration of EAB 515 from its free concentration determined in all the plasma ultrafiltrate samples.

Determination of Cortical ECF to Plasma and CSF to Plasma Ratio upon IV Administration of EAB 515

The microdialysate concentrations in all experiments were corrected for the probe recovery by the average of the RD recovery values over the duration of a particular experiment. The range of *in vivo* recovery values across probes, as

determined by RD, was 11.1% to 20.4% for the 2 mm length, and 6.1% to 15.1% for the 1 mm length. Within a given experiment, the RD loss of the calibrator was randomly variable with a coefficient of variation ranging from 6 to 20%, but did not show time dependent trends. This is shown for a typical rat in Figure 5. The profile of the average \pm S.D. of cortical ECF ($C_{\text{cortex,iv}}$) and CSF ($C_{\text{csf,iv}}$) concentrations of EAB 515 (corrected for *in vivo* recovery by RD) upon iv infusion in 12 rats is presented in Figure 6. The infusions were terminated at 900 min (15 hr). The average concentration in the two regions of the brain and in plasma for each animal during the last 3 hrs of the infusion are listed in Table I. The plasma concentrations were at a steady state after 6 hrs into the infusion. The concentrations of EAB 515 in the CSF were still increasing during the last few hours of iv infusion. However, the concentrations in the cortical ECF did not exhibit an increasing trend during the duration of the iv infusion. Figure 7 shows the ratio of average cortical and CSF concentrations in the 12 rats. Since the microdialysates from the two sites were analyzed during alternating 20 minute intervals, the values for the time-coincident intervals for each site were estimated by spline interpolation.

Determination of the Distribution Advantage in the Cortical ECF upon ICV Administration of EAB 515

The concentrations of EAB 515 in the FrC ECF ($C_{\text{cortex,icv}}$) at the end of a 15-hr constant-rate infusion (10 or 20 ng/min) of EAB 515 into the LV of the rats are listed in Table II. The icv infusion was either preceded or followed by an iv infusion (20–25 $\mu\text{g}/\text{min}$) of EAB 515 in the same animal with a washout period of at least 3 days between the two treatments. The incidence of ataxia and stereotyped behavior in the rats limited the icv infusion rates to no more than 0.1% of the iv infusion rates. EAB 515 concentrations in the cortical microdialysate were quantifiable within 1 hr of the start of icv infusion, and were corrected for probe recovery by the average *in vivo* RD recovery value. Figure 8 gives a comparative presentation of the time course of cortical levels of EAB 515 following iv and icv infusions of EAB 515, respectively. The cortical ECF concentrations at the end of iv and

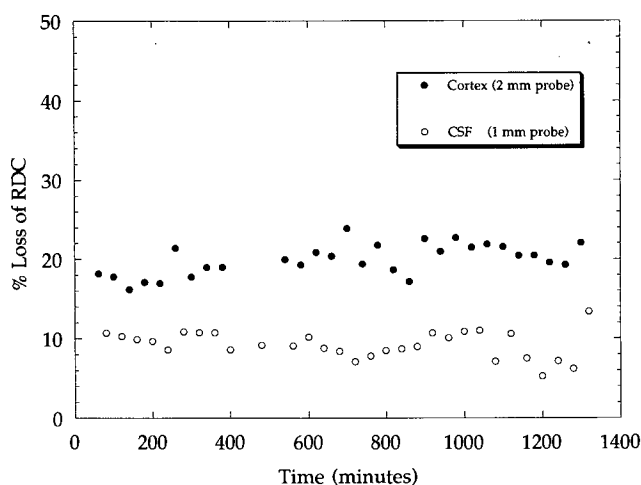


Fig. 5. The time-course of *in vivo* probe recovery as determined by retrodialysis, in the cortical ECF and CSF of a typical rat.

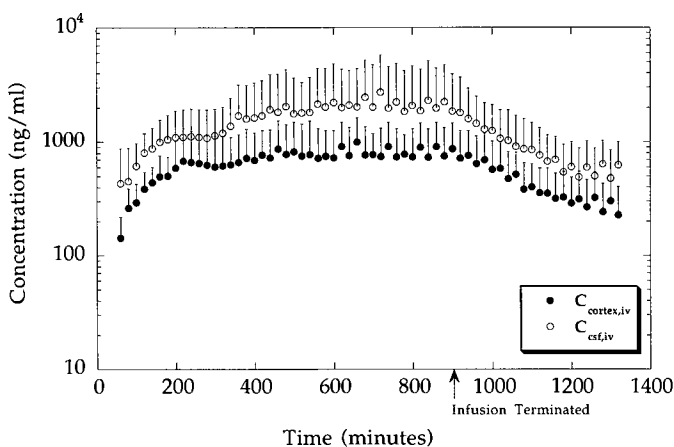


Fig. 6. Concentrations (average \pm S.D. of data from 12 rats) of EAB 515 in the frontal cortex and in the CSF following iv infusion of EAB 515. The infusion rates were 21–69 $\mu\text{g}/\text{min}$. All concentrations were corrected for probe recovery by RD method and normalized to an infusion rate of 25 $\mu\text{g}/\text{min}$.

icv infusions were normalized to a common infusion rate of 25 $\mu\text{g}/\text{min}$. The ratio of the normalized concentrations was computed to determine the distribution advantage upon icv infusion in each animal. In Figure 9, the cortical concentrations during the last 3 hrs of infusion have been plotted against the respective infusion rates for both iv and icv administrations.

Inhibition of the Facilitated Transport of EAB 515 by Probenecid

Table III lists the concentrations of EAB 515 in the plasma, cortex, and CSF during the control and probenecid treatment phases of the cross-over study. The ratio of the levels of EAB 515 during the two phases were examined in order to determine any possible interference of probenecid with the transport of EAB 515.

DISCUSSION

The results of *in vitro* retrodialysis indicated that RDC is a good calibrator for the determination of the recovery of EAB 515 in the *in vitro* microdialysis experiments. However, *in vivo* transport of the analyte and RD calibrator will be limited not by the probe membrane but by their respective microvasculature permeabilities, metabolism, cellular uptake, as well as diffusivity in the ECF and CSF. Therefore, the extension of the relationship determined *in vitro* between the loss of RDC and recovery of EAB 515 to an *in vivo* experiment requires further documentation. For this purpose simultaneous ZNF and RD based determination of probe recovery was conducted both *in vitro* and *in vivo*.

The successful application of ZNF *in vivo* requires the dialyzed tissue to be maintained at steady state with respect to the dialyzed solute. In a typical ZNF plot, the X-axis intercept is equivalent to a point of no net flux across the probe membrane and gives the steady-state concentration $C_{o,s}$ in the dialyzed medium. In a situation of increasing $C_{o,s}$ the X-axis intercept can be perceived as being continually shifted to the right. Where the order of consecutive perfusate changes involves an increase in $C_{i,s}$, this results in a regres-

Table I. EAB 515 Concentrations in the Cortex, CSF, and Plasma during IV Infusion

Rat	Ro	Cp,ss	C cort,iv**	C csf,iv**	C cort,iv/C p,ss	C csf,iv/Cp,ss	C cort,iv/C csf,iv
#	µg/min	µg/ml	ng/ml	ng/ml	%	%	%
A0	30	9.9	#	#	#	#	#
A1	69	16.3	540	#	3.3	#	#
A2	27	7.5	330	356	4.4	4.8	92.7
A3	33	7.0	617	2030	8.8	29.0	30.4
A4	21	7.7	282	1230	3.7	16.0	22.9
A5	21	8.5	350	1200	4.1	14.1	29.2
A6	21	8.5	1080	6560	12.7	77.2*	16.5
A7	24	7.9	817	2330	10.4	29.5	35.1
A8	21	12.8	4110	2920	32.0*	22.8	140.8
A9	22	9.4	892	2010	9.4	21.3	44.4
A10	23	7.7	817	1020	10.7	13.3	80.1
A11	23	8.4	421	1050	5.0	12.5	40.1
A12	23	10.0	1890	1410	18.9	14.1	134.0
AVG.					8.3	17.7	60.6
S.D.					4.8	7.8	44.5
%CV					58.1	44.0	73.5

* Value not used in computing average and S.D.

** average value during the last 3 hrs of the 15 hr iv infusion

quantities not measured

sion of the ZNF data providing a slope which underestimates the true recovery.

In the cortical site (see Figure 4a) there was good agreement between the recovery values determined by the two methods since the concentrations of EAB 515 in the cortex were not increasing during the performance of ZNF. However, the estimate of recovery by ZNF in the lateral ventricle (see Figure 4b) was almost half of the estimate obtained by simultaneous RD, presumably resulting from the violation of the steady-state assumption required by ZNF method. This is evident from the iv infusion studies where only RD was performed. It was noted that the concentration of EAB 515 in the CSF was progressively increasing during the 15-hr constant-rate infusion (see Figure 6).

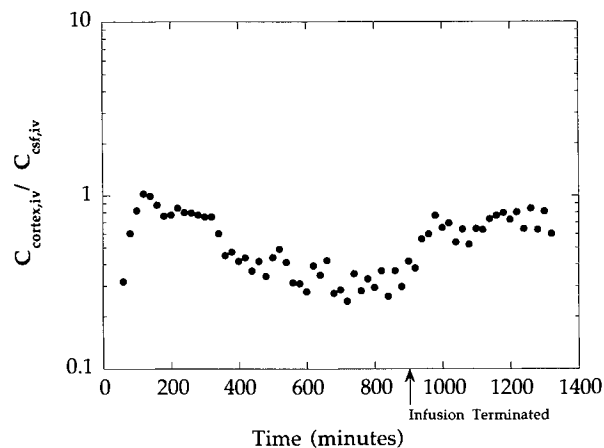


Fig. 7. Ratio of the average concentrations of EAB 515 in the frontal cortex and CSF following iv infusion of EAB 515.

In conclusion, the results obtained by RD and ZNF were comparable *in vitro* and *in vivo* in the frontal cortex, but not in the lateral ventricle. The reason for the discrepancy between the two methods in the CSF probably results from a violation of steady state requirement of ZNF, in the present experimental design. Therefore, in these studies, the use of a RD method of determining probe recovery was found to be suitable and more reliable than ZNF.

The process of RD introduces the calibrator into the tissue space surrounding the MD probe. After considering the MD perfusion rate, calibrator concentration in the perfusate, loss through the probe, and the turnover rate of CSF, it was estimated that the CSF concentration of RDC was no more than 2% of that in the perfusate and of that of EAB 515 in the CSF. This suggests that sink conditions exist for RDC outside the probe, and that interactions of RDC with the transport and/or metabolism of EAB 515 would be unlikely.

Relative to plasma, the concentration in the cortical ECF was found to be $8.3 \pm 4.8\%$ and that in the CSF was $17.7 \pm 7.8\%$ after 15 hrs of constant rate iv infusion. Studies of the spatial distribution of drugs in the brain (14) suggest that the high interanimal variability of these estimates may be due to small differences in probe placement within the cortex. The concentration of EAB 515 in the CSF did not attain a steady state during the 15 hrs of iv infusion of the drug. However, the cortical concentrations did not exhibit an increasing trend. The above observation is evident from the plot in Figure 7. During iv infusion while the concentrations in CSF are still increasing the ratio of cortical ECF to CSF concentrations continue to fall. In the post-infusion phase, initially the levels of EAB 515 in the CSF drop at a faster rate than they do in the cortex. This is followed by a parallel decline in cortex and CSF levels during the terminal

Table II. Distribution Advantage (DA) of EAB 515 in the FrC upon ICV Administration

Rat #	Riv	Ricv	C cort,iv	C cort,icv	C cort,iv/Riv	C cort,icv/Ricv	DA**
	$\mu\text{g}/\text{min}$	$\mu\text{g}/\text{min}$	ng/ml	ng/ml	min/ml	min/ml	
B1	33	0.01	617	186	0.019	18.6*	995*
B2	21	0.01	350	16	0.017	1.6	96
B3	21	0.01	1080	63	0.051	6.3	123
B4	24	0.01	817	37	0.034	3.7	109
B5	24	0.02	980	128	0.041	6.4	157
B6	24	0.02	869	145	0.036	7.3	200
AVG.					0.033	5.1	137
S.D.					0.013	2.3	42
%CV					40	46	31

* Value not used in computing the average and S.D.

** DA = (C cort,icv/Ricv)/(C cort,iv/Riv)

phase of elimination. This can also be observed in Figure 7, where the ratio of the two levels increase and approach a constant value in the post-infusion phase.

The cortical ECF and the CSF concentrations of EAB 515 during the last 3 hrs of the 15-hr iv infusion were only 8.3% and 17.7%, respectively, of the total steady-state concentration in the plasma. Since the extent of binding of EAB 515 in plasma is only 30%, the free concentrations in plasma were much higher than those in the CSF and in the cortical ECF. Although the cortical ECF and CSF concentrations were not truly at steady state, these results still indicate that passive processes alone may not be responsible for the transport of EAB 515 across the BBB and the BCB. Further, the concentrations in the CSF continued to increase throughout the 15 hrs of iv infusion. This may be explained by saturation of some facilitated efflux transport of EAB 515 from CSF to blood.

Figure 8 indicates the extent of increase in the levels of

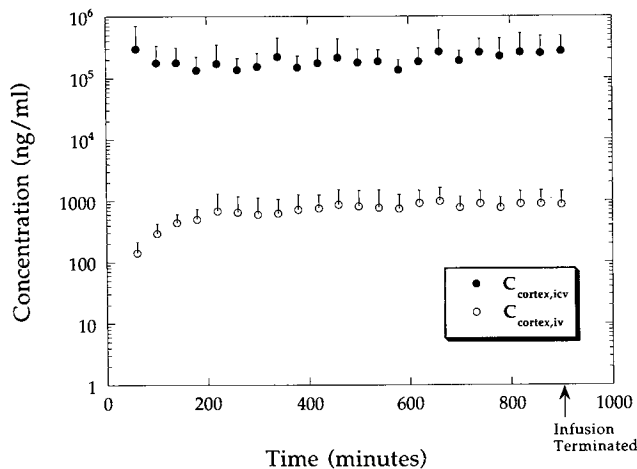


Fig. 8. Concentrations (average \pm S.D.) of EAB 515 in the frontal cortex following iv ($n = 12$) and icv ($n = 6$) administration of EAB 515. All concentrations are normalized to a 25 $\mu\text{g}/\text{min}$ infusion rate.

EAB 515 in the cortex when it was given by the icv route as opposed to the iv route. The levels in this Figure were normalized to a common 25 $\mu\text{g}/\text{min}$ rate of infusion for both the routes of administration, for purposes of comparison. In order to make a meaningful comparison after performing this normalization, it is assumed that EAB 515 follows linear elimination kinetics.

On a log-log scale, the $C_{\text{cortex,iv}}$ and $C_{\text{cortex,icv}}$ values should be linearly related to infusion rates, with a slope of unity. The vertical distance between these parallel lines provides a measure of the distribution advantage of the icv route over the iv route. Figure 9 demonstrates this, as it can be seen that the difference between the Y-intercepts of the two lines at any infusion rate, expressed as a logarithmic value, is equivalent to $\log DA$. The mean DA was found to be 136, as given in Table II. This suggests that a pathway for the transport of EAB 515 exists across the ependymal CSF-brain interface.

Because of the high contribution of flux from the CSF to the cortical site during icv administration, the spatial coordinates of the cortical probe become an important determinant of the measured value of DA for each animal. Post mortem histological examination of brain slices was performed to verify the probe placement in three animals. It was found that the ventricular guides were indeed positioned on the surface of LV, although the exact coordinates of the cortical guide could not be determined. It should be noted that the volumetric infusion rate employed for the icv route was only 15% of the CSF turnover rate reported in the literature (15). Intracerebroventricular infusion results in an increase in CSF absorption rate across the arachnoid villi, without affecting the CSF production rate (16).

One interpretation for the distribution advantage (DA) is that it represents the steady-state concentration (or concentration-time integral) of drug in a specific locus in the brain for a given mode (site) of administration relative to intravenous dosing, normalized to the administration rate (or dose). With reference to the model in Figure 1, if there exists a direct transport pathway between the site of administration

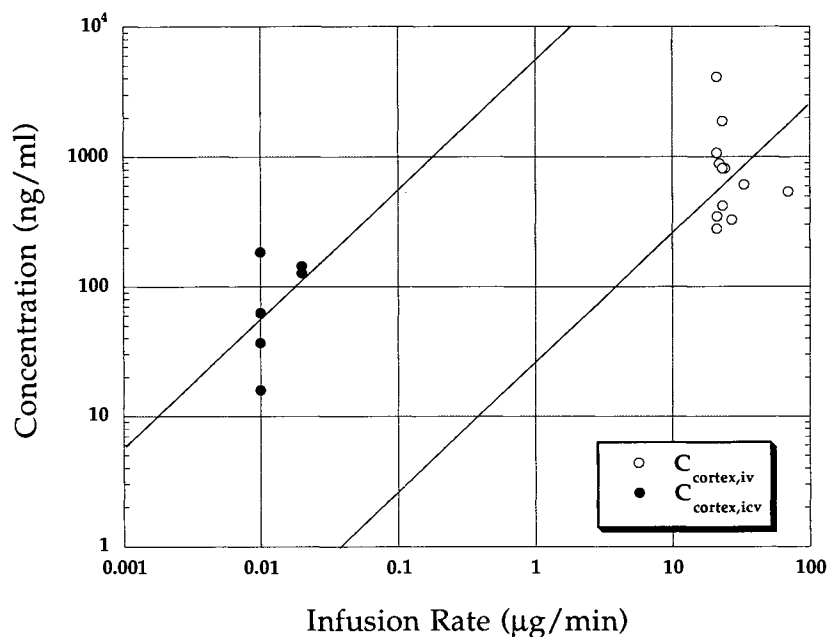


Fig. 9. Average concentration of EAB 515 in the frontal cortex during last 3 hrs of iv and icv administration. Each data point represents one rat.

and the brain locus (i.e., one that avoids passage through the central compartment), the DA will be greater than unity.

The model in Figure 1 also assumes that the central compartment is the only compartment responsible for elimination of the drug from the body. Thus, the site of administration (icv or iv) does not affect the drug concentration in the central compartment if identical infusion rates are utilized. In the present study icv infusion rates were maintained at low levels due to the stereotyped behavior and ataxia exhibited by the rats during infusion of EAB 515. It was estimated that plasma concentrations of EAB 515 would be less than 10 ng/ml at infusion rates of 20 ng/min in a typical rat, assuming that the brain did not act as an organ of first-

pass metabolism of EAB 515, and that linear elimination kinetics were obeyed. Since this concentration was below the minimum quantifiable limit, we were unable to measure the concentrations of EAB 515 in plasma following icv administration, and could not verify the preceding assumption.

The total body clearance of EAB 515, determined as a ratio of the steady state plasma concentrations and the respective iv infusion rates, was found to be $8.5 (\pm 1.6)$ ml/min/kg for rats. Preliminary studies in the rabbit (unpublished data from our laboratory) have indicated that the renal excretion of EAB 515 is responsible for over 90% of its total body clearance. Plasma ultrafiltrates following iv administration of EAB 515 in rats and in rabbits have not demon-

Table III. EAB 515 Concentrations in Cortex, CSF, and Plasma after Control and Probenecid Treatments

Rat	Riv	C p,ctrl	C p,pbd	C cort,ctrl	C cort,pbd	C csf,ctrl	C csf,pbd	Plasma	Cort	CSF
#	µg/min	µg/ml	µg/ml	ng/ml	ng/ml	ng/ml	ng/ml	pbd/ctrl	pbd/ctrl	pbd/ctrl
C1	24	9.1	14.5	980	1060	544	966	1.60	1.08	1.78
C2	25	9.0	15.0	368	370	2510	3400	1.67	1.01	1.35
C3	25	8.7	15.4	650	759	830	1340	1.77	1.17	1.61
C4	24	7.7	13.1	558	528	4190	6620	1.70	0.95	1.58
C5	24	7.5	13.9	869	2090	1740	3080	1.85	2.41*	1.77
C6	25	8.1	13.8	529	607	1350	2140	1.71	1.15	1.59
AVG.								1.72	1.05	1.62
S.D.								0.09	0.10	0.17
%CV								6	9	11

* value not included in computing average and S.D.

ctrl: control; pbd: probenecid treatment

PBD was infused at 75 µg/min to target a probenecid concentration of approx. 200 µg/ml in plasma

strated any metabolite peaks under the chromatographic conditions of plasma analysis. This suggests that in the rat also it is possible that the clearance value of 8.5 ml/min/kg may be a result of renal excretion of the drug alone. The glomerular filtration rate (GFR) in the rat is 5.2 ml/min/kg (12). The free fraction of EAB 515 in plasma of rats was found to be 0.7. Thus, the renal filtration process (expressed as $fu \cdot GFR$ and equal to 3.6 ml/min/kg) accounts for less than half of the total body clearance of EAB 515. This would suggest the involvement of a significant secretory component in the renal excretion of EAB 515.

Probenecid has been shown to compete with compounds structurally similar to EAB 515 for facilitated transport pathways (13). For AZT, probenecid has been shown to inhibit the renal secretory transport as well as the facilitated transport of AZT from the brain into the systemic circulation (5,17,18).

Table III shows that during probenecid coadministration, the total body clearance of EAB 515 was decreased by 42%. This may be due entirely to inhibition of renal secretory transport of EAB 515. However, further renal clearance studies in the rat are required to support this argument. The levels of EAB 515 in the CSF were also increased to a similar extent as in the plasma during probenecid treatment. This suggests that probenecid had no effect on the transport kinetics of EAB 515 across the blood-CSF barrier.

Probenecid treatment (in five out of six rats studied) resulted in a 38% reduction in cortical to plasma ratios of EAB 515 relative to their control periods. Although this observation suggests that probenecid may inhibit the transport of EAB 515 from blood into cortical ECF, this appears to be inconsistent with other findings. For example, the BUI for EAB 515 was reported to be only 2%, and the permeability coefficient of EAB 515 (computed from two *in vitro* models of BBB) was similar to that of sucrose across the BBB (19). Based upon this study, the authors concluded that even though EAB 515 can inhibit the brain penetration of L-phenylalanine, the passage of EAB 515 itself through the BBB is not appreciable, and probably not carrier-mediated.

The results of the present study indicate that coadministration of probenecid with EAB 515 would not offer any advantage in increasing uptake of EAB 515 into cortical tissue. Although it could be argued that probenecid may have the potential to reduce cortical uptake where this is desirable, further studies would be needed to examine the effects of probenecid on the brain distribution of EAB 515 and related NMDA antagonists.

ACKNOWLEDGMENTS

Support for this work was provided by Sandoz Pharma Ltd., Basel, Switzerland. The authors are grateful for the helpful suggestions provided by J. F. Brouillard of Sandoz Pharma Ltd., Basel, concerning the HPLC analysis of EAB 515 in plasma. Technical help was provided by Linda Cartier, Jill Maloney, and Richard Brundage of the Department of Pharmaceuticals, University of Minnesota, and by Pierrette Misslin of Sandoz Pharma Ltd., in the development of the freely moving rat model used in this study.

REFERENCES

1. K. A. O'Neill and J. M. Liebman. Unique behavioral effects of NMDA antagonist, CPP, upon injection into the medial prefrontal cortex of rats. *Brain Res.* 435:371-376 (1987).
2. D. T. Monaghan and C. W. Cotman. Distribution of NMDA sensitive L-[³H]-glutamate binding sites in the rat brain. *J. Neurosci.* 11:2909-2919 (1985).
3. W. Muller, D. A. Lowe, H. Neijt, S. Urwyler, and P. Herrling. Synthesis and N-methyl-D-aspartate (NMDA) antagonist properties of the enantiomers of α -amino-5(phosphonomethyl)[1,1'-biphenyl]-3-propanoic acid. Use of a new chiral glycine derivative. *Hel. Chim. Act.* 75: 855-864 (1992).
4. W. M. Pardridge. Strategies for directed drug delivery through the blood-brain barrier. In R. T. Borhardt, A. J. Repta, and V. J. Stella (eds.), *Directed Drug Delivery*, Humana Press, Clifton NJ, 1985, pp. 83-96.
5. S. L. Wong, K. V. Belle, and R. J. Sawchuk. Distributional transport kinetics of zidovudine between plasma and brain extracellular fluid in the rabbit: Investigation of the inhibitory effect of probenecid utilizing microdialysis. *J. Pharmacol. Exp. Ther.* 264: 899-909 (1993).
6. I. Jacobson, M. Sandberg, and A. Hamberger. Mass transfer in brain dialysis devices: a new method for the estimation of extracellular amino acids concentration. *J. Neurosci. Meth.* 15: 263-268 (1985).
7. P. Lonroth, P. A. Jansson, and U. Smith. A microdialysis method allowing characterization of intercellular water space in humans. *Am. J. Physiol.* 253: E228-231 (1987).
8. Y. F. Wang, S. L. Wong, and R. J. Sawchuk. Comparison of *in vitro* and *in vivo* calibration of microdialysis probes using retrodialysis. *Curr. Separ.* 10:87 (1991).
9. Y. F. Wang, S. L. Wong, and R. J. Sawchuk. Microdialysis calibration using retrodialysis and zero-net flux: Application to a study of the distribution of zidovudine to rabbit CSF and thalamus. *Pharm. Res.* 10:1411-1419 (1993).
10. C. Kozma, W. Macklin, L. M. Cummins, and R. Mauer. The anatomy, physiology, and biochemistry of the rabbit. In S. H. Weisbroth, R. E. Flatt and A. L. Kraus (eds.), *The Biology of the Laboratory Rabbit*, Academic Press, New York, 1974, pp. 49-72.
11. G. Paxinos and C. Watson. *The Rat Brain in Stereotaxic Coordinates*, Academic Press, Inc., California, 1986.
12. B. Davies and T. Morris. Physiological parameters in laboratory animals and humans. *Pharm. Res.* 7:1093-1095 (1993).
13. L. Vecsei, J. Miller, U. MacGarvey, and M. F. Beal. Kynurenine and probenecid inhibit pentylenetetrazol- and NMDA-induced seizures and increase kynurenine acid concentrations in the brain. *Brain Res. Bull.* 28:233-238 (1992).
14. K. H. Dykstra, A. Arya, D. A. Arriola, P. M. Bungay, P. F. Morrison, and R. L. Dedrick. Microdialysis study of zidovudine (AZT) transport in rat brain. *J. Pharmacol. Exp. Ther.* 267: 1227-1235 (1993).
15. W. M. Pardridge. Transnasal and intraventricular delivery of drugs. In W. M. Pardridge (ed.), *Peptide Drug Delivery to the Brain*, Raven Press, New York, 1991, pp. 114-116.
16. G. A. Rosenberg. Physiology of cerebrospinal and interstitial fluids. In G. A. Rosenberg (ed.), *Brain Fluids and Metabolism*, Oxford University Press, New York, 1990, pp. 37-42.
17. M. A. Hedaya, W. F. Elmquist, and R. J. Sawchuk. Probenecid inhibits the metabolic and renal clearances of zidovudine (AZT) in plasma and urine. *Clin. Chem.* 34:1565-1568 (1988).
18. M. A. Hedaya and R. J. Sawchuk. Effect of probenecid on the renal and non-renal clearances of zidovudine and its distribution into cerebrospinal fluid in the rabbit. *J. Pharm. Sci.* 78:716-722 (1989).
19. M. P. Dehouck, F. Guillot, C. Schluep, M. Lemaire, and C. Cecchelli. The Blood Brain Barrier *in vitro*. Comparison between a primary culture of brain microvessel endothelial cells and a coculture of brain capillary endothelial cells and astrocytes. Submitted for publication in *Eur. J. Pharmacol.*